JOURNAL OF MATERIALS SCIENCE 21 (1986) 4436–4442

Kinetics and mechanism of ferrous spinel oxidation studied by electrical conductivity and thermogravimetry

B. GILLOT, F. JEMMALI
Laboratoire de Recherches sur la Réactivité des Solides UA 23, Faculté des Sciences Mirande, BP 138, 21004 – Dijon Cedex, France

A. ROUSSET
Laboratoire de Chimie des Matériaux Inorganiques, Université Paul Sabatier, Toulouse III, 118 route de Narbonne, 31000 Toulouse, France

A mechanism of valence transfer between Fe^{2+} and Fe^{3+} ions in the octahedral, as well as the tetrahedral position of the spinel lattice is suggested to account for the electrical behaviour with the number of Fe^{2+}–Fe^{3+} pairs in either position for oxidation reactions in finely-grained ferrous spinels. From the $\sigma = f(t)$ curves which are identified with those obtained in thermogravimetry, it was established for inverse spinels such as Fe_3O_4 or for normal spinels such as $FeCr_2O_4$ that the kinetics is governed by a diffusion law under variable working conditions. For more complex spinels such as chromium- or titanium-substituted magnetites which exhibit both Fe^{2+} ions on octahedral and tetrahedral sites, the results are discussed only qualitatively although the profile of the $\sigma = f(t)$ curves can also be related to the electronic exchange between the Fe^{2+} and Fe^{3+} ions from the two cation sites.

1. Introduction

The behaviour in oxygen of finely grained ferrous spinels has been studied in this laboratory over the past few years. These spinels, whose crystallite size is less than about 200 nm, could be oxidized to defect phase γ with the same spinel structure. The oxidation performed by electrical conductivity or thermogravimetry [1] indicates that the necessary temperature for oxidizing the Fe^{2+} to Fe^{3+} ions increases from spinel-like magnetite where all Fe^{2+} ions are on octahedral sites (most oxidation temperatures are in the range 150 to 250° C) to spinel-like iron chromite or aluminate where all Fe^{2+} ions are on tetrahedral sites (most oxidation temperatures are in the range 400 to 500° C). This discrepancy of reactivity between ferrous ions has been attributed to the fact that ions in the tetrahedral sites are strongly bound by covalent bonds, in contrast to the ionic bonding of octahedrally sited ions.

In thermogravimetry the oxidation process always exhibits an increase of weight gain whatever the location of Fe^{2+} ions because during oxidation, oxygen atoms adsorbed on the grain surface become ionized by acquiring electrons from Fe^{2+} ions diffusing through the crystal. The process was solely limited by bulk ionic diffusion, which must be considered under variable working conditions. On the other hand, in electrical conductivity the conduction mechanism can be envisaged as an electron "hopping" between Fe^{2+} and Fe^{3+} ions as $Fe^{3+} \rightleftharpoons Fe^{2+} + e$ and this valence transfer may exist in octahedral (B sites) as well as in tetrahedral sites (A sites). Inverse spinels such as magnetite or magnetites substituted by divalent cations (Co^{2+}, Zn^{2+}), with a high initial conductivity undergo a large conductivity decrease during oxidation, related to the generation of Fe^{3+} ions and vacancies on B sites, upsetting the electron exchange between the Fe^{2+} and Fe^{3+} ions initially present in equal amounts. Alternatively, normal spinels such as iron aluminate, iron chromite, solid solution $FeCr_2O_4$–$FeAl_2O_4$ or highly chromium-substituted magnetites, exhibit an initial increase in conductivity. This is due to the simultaneous presence of Fe^{2+} and Fe^{3+} ions on A sites, which allows electron exchange between cations on equivalent sites. Then, when Fe^{3+} ions prevail, the conductivity decreases until the γ compound is obtained. These observations have been confirmed recently for more complex spinels such as aluminium- or chromium-substituted magnetites [2] whose substitution ratio x is in the composition range $0.4 < x < 1.80$ or as titanomagnetites which exhibit both Fe^{2+} ions on B and A sites [3].

The purpose of this paper is to develop a theoretical model of diffusion which describes for the first time, the different possibilities of electron exchange that the location of Fe^{2+} ions in spinel structure introduces during oxidation at low temperature. If such a model is coupled with respect to the diffusion laws established by thermogravimetry from isothermal oxidations, then such a model may explain the electical behaviour according to the nature of the spinel and as a function of oxidation extent. To this end, Section 2 summarizes some of the experimental results obtained from electrical and thermogravimetric measurements in

0022–2461/86 $03.00 + .12

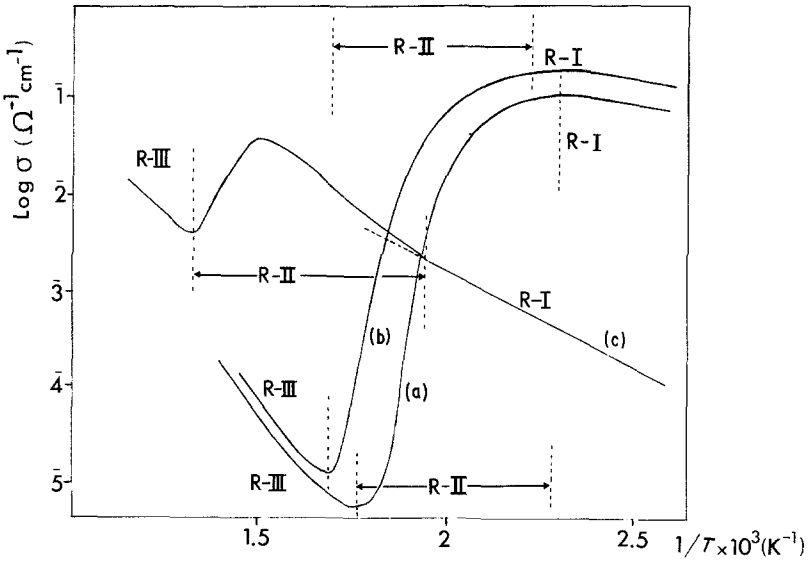

Figure 1 Evolution of electrical conductivity with temperature during oxidation in defect phases γ. (a) Fe_3O_4; (b) zinc-substituted magnetite with $x = 0.69$; (c) $FeCr_2O_4$.

non-isothermal and isothermal conditions for oxidation of ferrous iron from the two cations sites of the spinel structure. Fe^{2+}-bearing spinels were selected in which the Fe^{2+} ion was located principally either on one sublattice or the other.

The preparation of samples and experimental procedure concerning the oxidation in defect phases γ have already been reported [4–7].

2. Study by electrical conductivity and thermogravimetry of oxidation of ferrous spinels

2.1. Non-isothermal method

The behaviour of electrical conductivity during oxidation of Fe^{2+} ions is shown in Fig. 1 for ferrous spinels in which the Fe^{2+} ion is predominantly in either the B (Figs 1a and b) or the A sites (Fig. 1c). Generally, for temperatures below 500° C, three regions can be distinguished.

(i) In region I, the conductivity of the initial phase increases with increase of temperature and in all cases the compounds show a semi-conducting behaviour.

(ii) Region II is due to the oxidation of Fe^{2+} ions. The zinc-substituted magnetites of structural formula $(Zn_x^{2+}\,Fe_{1-x}^{3+})_A(Fe_{1+x}^{3+}Fe_{1-x}^{2+})_BO_4^{2-}$ $(0 < x < 1)$ with Fe^{2+} ions on the B sites (Figs 1a and b) show a large decrease of conductivity with increase of temperature. This can be explained by a decrease of Fe^{2+} ions with increasing value of the number of vacancies in B sites, and consequently a decrease of Fe^{2+}–Fe^{3+} pairs, because the created vacancies do not contribute to the conductivity.

For iron chromite $(Fe^{2+})_A(Cr_2^{3+})_BO_4^{2-}$, an initial increase of conductivity is observed due to the formation through oxidation of Fe^{3+} ions on A sites which favours electron "hopping" on these sites (Fig. 1c). Maximum conductivity appears approximately when the amount of Fe^{2+} and Fe^{3+} ions on A sites is equal. Then, when the amount of Fe^{3+} ions is large, the conductivity decreases as in the case of zinc-substituted magnetites.

(iii) Finally, in region III the electrical conductivity increases with increase in temperature according to the negative temperature coefficient of defect phases γ.

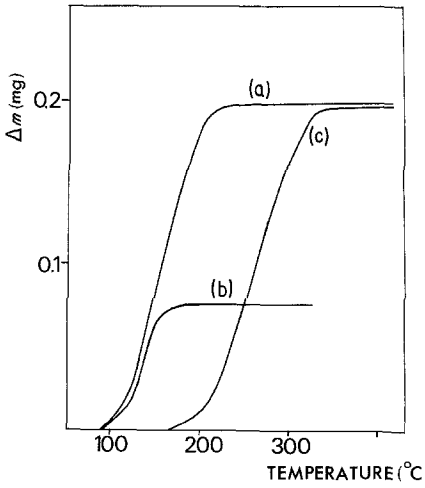

Figure 2 TG curves showing the weight gain. (a) Fe_3O_4; (b) zinc-substituted magnetite with $x = 0.69$; (c) $FeCr_2O_4$.

If in region II, the electrical conductivity is a structurally sensitive physical parameter to characterize the process of oxidation of Fe^{2+} ions, thermogravimetry is not of such interest because, as shown in Fig. 2, oxidation is always accompanied by a weight gain, Δm, in direct relation to the Fe^{2+} content. For comparison we have also reported a weight gain for pure magnetite.

2.2. Isothermal method

The oxidations performed under isothermal conditions in region II confirm the influence of cation distributions on electrical conductivity. From the experimental results reported in Figs 3, 4 and 5 for different spinels and an initial oxygen pressure of 10^2 Pa, it appears that the change in the number of Fe^{2+}–Fe^{3+} pairs largely affects the electrical behaviour. For zinc-substituted magnetites (Fig. 3) the $\sigma = f(t)$ curves show a rapid decrease in conductivity with time, while for chromium-substituted magnetites $Fe_{3-x}Cr_xO_4$ with $x \geqslant 1.80$ (Fig. 4) or for $FeCr_2O_4$–$FeAl_2O_4$ solid solutions (Fig. 5) the $\sigma = f(t)$ curves display very different behaviour with a clearcut maximum.

From a network of $\sigma = f(t)$ curves for zinc-substituted magnetites with $x = 0.69$, we have plotted the $\alpha' = f(t)$ curves (Fig. 6), α' being the transformation extent defined by $\alpha' = \sigma_{(t)} - \sigma_{(f)}/\sigma_{(o)} - \sigma_{(f)}$

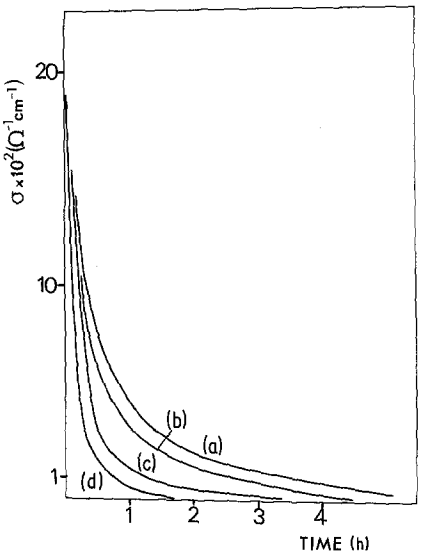

Figure 3 Evolution of conductivity with time for zinc-substituted magnetites with (a) $x = 0.18$, $T = 160°C$; (b) $x = 0.33$, $T = 185°C$; (c) $x = 0.69$, $T = 235°C$; (d) $x = 0.90$, $T = 290°C$.

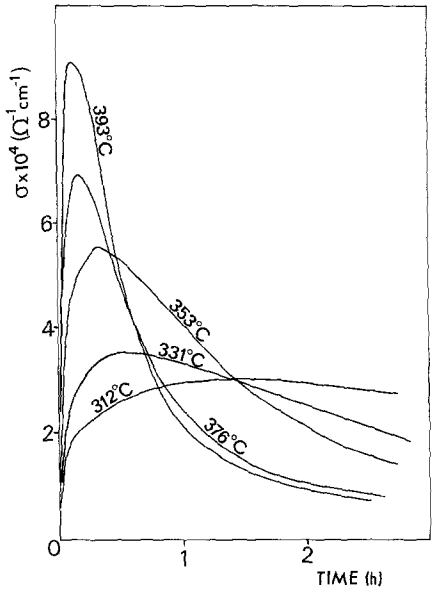

Figure 5 Evolution of conductivity with time for spinel $(Fe^{2+}Al^{3+}_{0.5}-Cr^{3+}_{1.5})O^{2-}_4$.

where: $\sigma_{(o)}$ is the conductivity in vacuum at the given temperature, $\sigma_{(t)}$ is the conductivity at time t and $\sigma_{(f)}$ is the conductivity of the defect phase γ (totally oxidized product). These curves can be superimposed in an affinity versus time. On the other hand, the curves $\theta = f(t)$ resulting from the transformation $1 - \alpha'_{(t)}$ (Fig. 7) are very similar to the $\alpha = f(t)$ curves obtained in thermogravimetry by recording the weight gain corresponding to oxygen fixation (α is determined by the ratio of partial oxidation weight gain to complete oxidation weight gain). In both thermogravimetry and conductivity the curves are practically superimposable whatever the composition. Thus we can deduce that the weight change recorded in the thermobalance and the conductivity change resulting from the number of $Fe^{2+}-Fe^{3+}$ pairs reflect the same kinetic laws. However, a such similarity does not exist for ferrous spinels with Fe^{2+} ions on A sites since, as already mentioned, these spinels exhibit a different electrical behaviour although no anomaly appears in the $\alpha = f(t)$ curves recorded in the thermobalance where the oxidation reaction also resulted in an increase of sample mass. Finally, the kinetics of weight gain contribute to the variation of number of $Fe^{2+}-Fe^{3+}$ pairs and affects the conductivity of two different ways. In the case of pure magnetite and magnetites substituted by divalent cations (Zn^{2+}, Co^{2+}), the weight gain requires a decreasing of number of $Fe^{2+}-Fe^{3+}$ pairs, whereas for iron chromite, iron aluminate or $FeCr_2O_4-FeAl_2O_4$ solid solutions the initial weight gain is associated with an increasing number of $Fe^{2+}-Fe^{3+}$ pairs up to $\alpha = 0.5$, then for $\alpha > 0.5$ it is associated with a decrease of $Fe^{2+}-Fe^{3+}$ pairs.

To verify this we have studied oxidation as a function of time for various, already partially oxidized spinels $(Fe^{2+})_A(Al^{3+}_{2-x}Cr^{3+}_x)O^{2-}_4$ with $x = 1.5$ and whose oxidation extent α is known (Fig. 8). As might be expected, the conductivity increases initially with time if $\alpha < 0.5$, and it decreases from the very beginning if $\alpha > 0.5$. For each conversion rate, α, we have also determined the activation energy, E, from the slope of the straight lines $\log \sigma = f(1/T)$ (Fig. 9). The minimum of E for α close to 0.5 results from the fact that for that α value, the Fe^{2+} and Fe^{3+} ions are equally distributed on A sites and this means that the

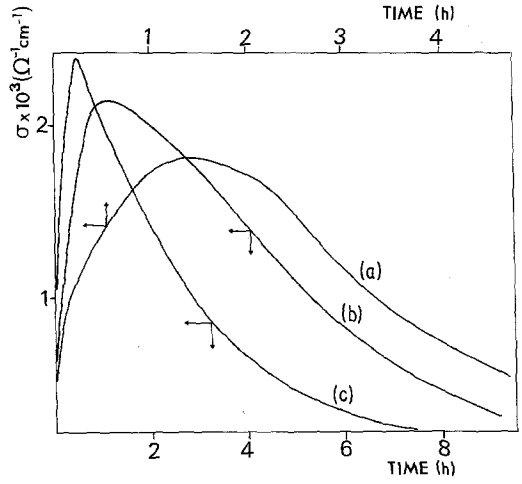

Figure 4 Evolution of conductivity with time for chromium-substituted magnetites with (a) $x = 2$, $T = 355°C$; (b) $x = 1.80$, $T = 330°C$; (c) $x = 1.80$, $T = 354°C$.

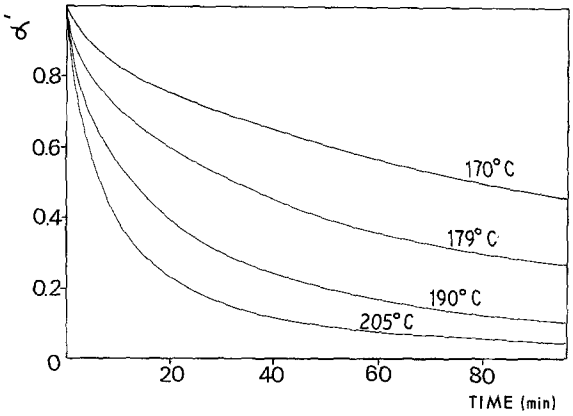

Figure 6 $\alpha' = f(t)$ curves for zinc-substituted magnetite with $x = 0.69$.

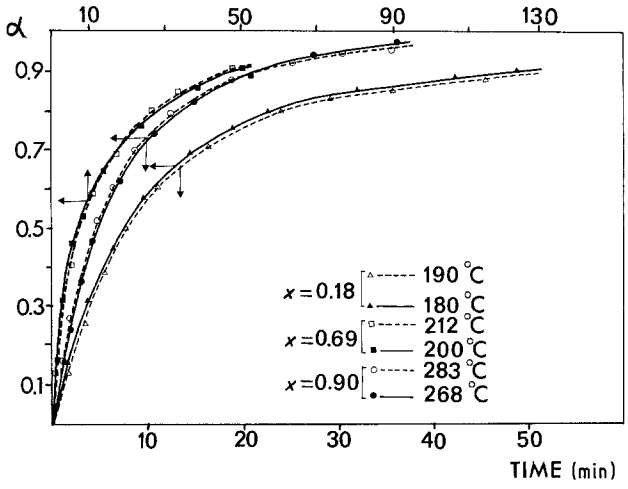

Figure 7 Analogy between the $\alpha = f(t)$ curves obtained by thermogravimetry and $(1 - \alpha') = f(t)$ curves obtained by electrical conductivity for zinc-substituted magnetites.

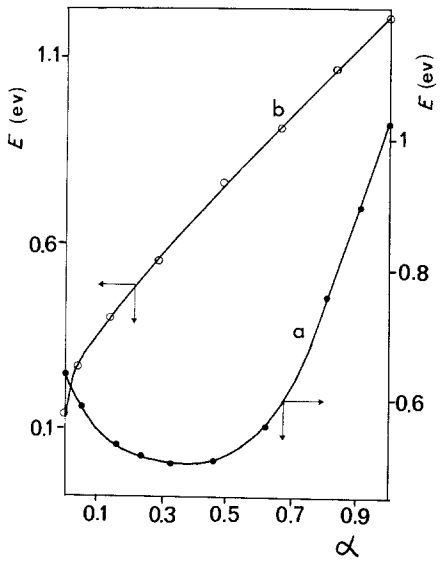

Figure 9 Evolution of activation energy with conversion rate, α. (a) Normal spinel $(FeAl_{0.5}Cr_{1.5})O_4$; (b) inverse spinel Fe_3O_4.

electron exchange is maximum. In contrast, in the case of pure magnetite, E increases continually with increasing of α (Fig. 9). On the other hand, recent studies by the Mössbauer spectroscopy [8] have shown for iron chromite with $\alpha = 0.5$, the possibility at $T > 440$ K, for a part of iron to display a mixed valence character due to a fast electron relaxation between Fe^{3+} and Fe^{2+} ions situated at A sites.

The possible connection between weight gain and number of Fe^{2+}–Fe^{3+} pairs is based on the observation that both are common to oxidation reactions and were observed under similar conditions. From these data, a diffusion mechanism was suggested to account for the possible relation between conductivity behaviour and kinetics laws obtained in thermogravimetry.

3. Oxidation mechanism

Using Kröger's notation [9] we have already shown [10] that the elementary steps in the oxidation of ferrous spinels to defect phase γ, including both the interfacial (adsorption and electron transfer) and diffusion steps will be expressed as follows:

$$\tfrac{1}{2}O_{2(g)} + Fe_{Fe_{II(surf)}} \rightleftarrows Fe_{\overline{Fe_{II(surf)}}O} \quad (1)$$

$$Fe_{\overline{Fe_{II(surf)}}O} + 2Fe_{Fe_{II}} \rightleftarrows Fe_{Fe_{II(surf)}} + \tfrac{1}{4}V''_{Fe_{Fe_{II}}} + \cdots + \tfrac{1}{2}V'''_{Fe_{Fe_{II}}} + 2Fe^{\cdot}_{Fe_{II}} + O_0 \quad (2)$$

diffusion: Fick's law (3)

The rate determining step was shown to be diffusion [10] which must be considered under variable working conditions ($\delta c/\delta t \neq 0$). No solid–solid phase boundaries are present and the process may be considered as an interdiffusion within the oxide itself with a consequent change of stoichiometry. The concentration distribution is given by Fick's second law:

$$\frac{\delta c}{\delta t} = D\left(\frac{\delta^2 c}{\delta r^2} + 2\frac{\delta c}{\delta r}\right) \quad (4)$$

In order to determine the boundary conditions we have established a correspondence between the weight change (diffusion) and evolution of Fe^{2+}–Fe^{3+} pairs contributing to conductivity for two spinels: Fe_3O_4 (Fe^{2+} ions on B sites) and $FeCr_2O_4$ (Fe^{2+} ions on A sites).

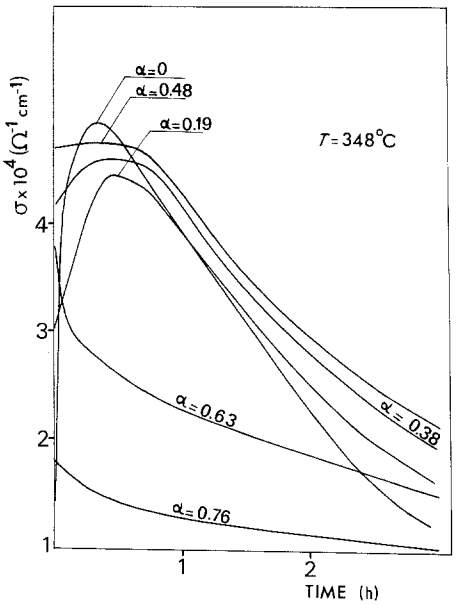

Figure 8 Evolution of electrical conductivity with time for different oxidation extents, α: $(Fe^{2+}Al^{3+}_{0.5}Cr^{3+}_{1.5})O^{2-}_4$.

3.1. Case of magnetite: inverse spinel $(Fe^{3+})_A(Fe^{2+}Fe^{3+})_BO^{2-}_4$

At $t = 0$ and for a concentration C_0 of Fe^{2+} ions, the number of Fe^{2+}–Fe^{3+} pairs is maximum and the number of Fe^{2+} ions is equal to the number of Fe^{3+} ions (Fig. 10a).

At $t > 0$ a fraction of the Fe^{2+} cations diffuse at the crystal surface, producing new Fe^{3+} cations which affects the mechanism of electron "hopping" between Fe ions on B sites since the number of Fe^{2+}–Fe^{3+} pairs decreases (Fig. 10b). Thus, the number of Fe^{2+}–Fe^{3+} pairs varies with the concentration of Fe^{2+} ions remaining in the interior of the grain. With the following boundary conditions

$$t = 0 \quad C_{(r)} = C_0 \quad \text{for } 0 \leqslant r \leqslant a$$

$$t > 0 \quad C = 0 \quad \text{for } r = a$$

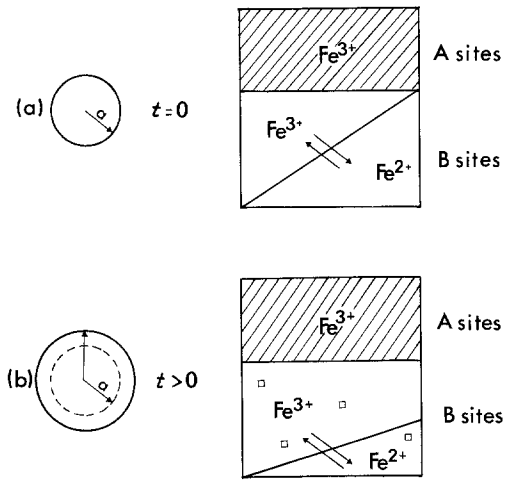

Figure 10 Schematic illustration of the various Fe^{2+}–Fe^{3+} "hopping" possibilities (↑↓) on B sites. (□) Vacancies. (a) $t = 0$; (b) $t > 0$.

and for spherical particles of radius a, the concentration, C, of cationic vacancies associated with positive holes linked to iron cations can be expressed as:

$$C(r, t) = -\frac{2aC_0}{\pi r}\sum_{n=1}^{\infty}\frac{(-1)^n}{n}\sin\frac{n\pi r}{a}e^{-n^2kt} \quad (5)$$

$$\text{with} \quad k = \frac{\pi^2}{a^2}\tilde{D}$$

where a is the mean grain radius and $\tilde{D}$ the chemical diffusion coefficient. The above solution of the problem gives the connection in terms of time and location (r). An equation given the fraction α' at any time is more suitable and is described by [11]:

$$\alpha' = \frac{\sigma_{(t)} - \sigma_\infty}{\sigma_0 - \sigma_\infty} = \frac{Q'(t)}{Q'_0} = \frac{6}{\pi^2}\sum_{n=1}^{\infty}\frac{1}{n^2}e^{-n^2kt} \quad (6)$$

where $Q'(t)$ = amount of matter remaining in the grain at time t and Q'_0 is the amount at $t = \infty$. Thus the reaction kinetics observed in electrical conductivity is given by Equation 6.

The comparison of this expression with that obtained from weight change measurements [12]

$$\alpha = 1 - \frac{6}{\pi^2}\sum_{n=1}^{\infty}\frac{1}{n^2}e^{-n^2kt} \quad (7)$$

leads to the relation previously determined from kinetics curves $\alpha = 1 - \alpha'$.

3.2. Case of iron chromite: normal spinel $(Fe^{2+})_A(Cr_2^{3+})_BO_4^{2-}$

At $t = 0$ and for a concentration C_0 of Fe^{2+} ions, the number of Fe^{2+}–Fe^{3+} pairs on A sites exchanging a mobile electron is zero (Fig. 11a).

For $0 < t < t_0$, the number of Fe^{2+}–Fe^{3+} pairs contributing to the conductivity is equal to the number of Fe^{3+} cations resulting from oxidation of an amount of Fe^{2+} ions which have diffused during time t, that is $0 < t < t_0$ (Fig. 11b).

For $t = t_0$, equality between Fe^{3+} and Fe^{2+} ions is obtained and electronic exchange is maximum (Fig. 11c). Thus, for $0 < t < t_0$, it is the diffusion outside the grains of Fe^{2+} cations that is responsible for the evolution of the number of pairs.

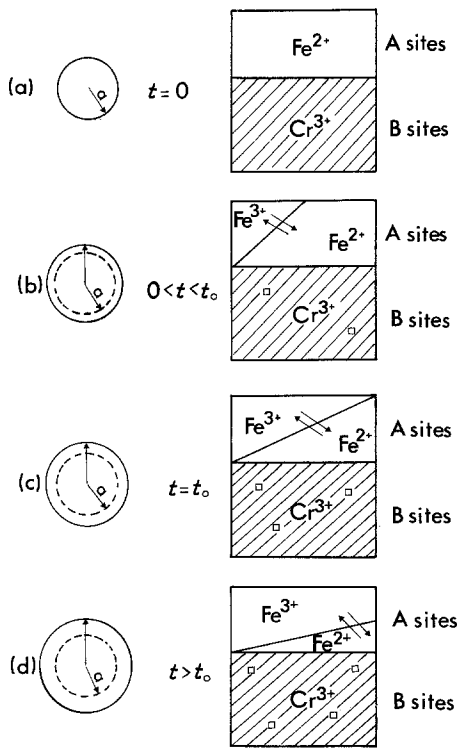

Figure 11 Schematic illustration of the various Fe^{2+}–Fe^{3+} "hopping" possibilities (↑↓) on A sites. (□) Vacancies. (a) $t = 0$; (b) $0 < t < t_0$; (c) $t = t_0$; (d) $t > t_0$.

For $t \geqslant t_0$, diffusion towards the crystal surface of Fe^{2+} cations reduces the number of pairs, as in the case of pure magnetite (Fig. 11d).

From these considerations the initial and boundary conditions are:

$t = 0$	$C_{(r)} = C_0$	for $0 \leqslant r \leqslant a$
$0 < t < t_0$	$C = C_1$	for $r = a$
$t = t_0$	$C_{(r)} = C_1$	for $0 \leqslant r < a$
$t_0 < t < t_\infty$	$C_{(r)} = 0$	for $r = a$

For $t = 0$ and $0 < t < t_0$, the concentration C can be written as:

$$C_{(r,t)} = C_1 - \frac{2a(C_0 - C_1)}{\pi r}\sum_{n=1}^{\infty}\frac{(-1)^n}{n}\sin\frac{n\pi r}{a}e^{-n^2kt} \quad (8)$$

In considering the amount of water diffusing through the surface of the grain at time t:

$$Q_t = 4\pi a^2\int_0^t -D(\delta c/\delta r)_{r=a}dt \quad (9)$$

this expression can be written as:

$$Q_{(t)} = 4/3\pi a^3(C_0 - C_1)\left[1 - \frac{6}{\pi^2}\sum_{n=1}^{\infty}\frac{1}{n^2}e^{-n^2kt}\right] \quad (10)$$

Thus, for $0 < t < t_0$, the kinetics observed in electrical conductivity $\sigma_{(t)}$ is given by Equation 10.

For $t_0 < t < t_\infty$, these kinetics are described as in the case of magnetite by:

$$\sigma'_{(t)} = \frac{8a^3C_1}{\pi}\sum_{n=1}^{\infty}\frac{1}{n^2}e^{-n^2kt} \quad (11)$$

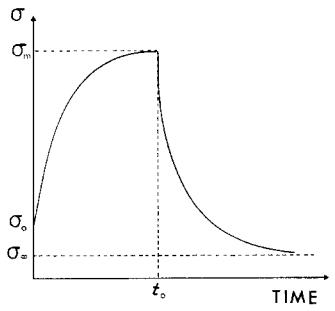

Figure 12 Schematic illustration of the evolution of electrical conductivity with oxidation time of spinel $(Fe^{2+})_A(Cr_2^{3+})_BO_4^{2-}$.

The kinetics observed in conductivity for iron chromite appears to depend on the simultaneous presence of $Fe^{2+}-Fe^{3+}$ pairs on A sites and undergoes two laws of diffusion with a transition for $t = t_0$. This transition corresponds to equal numbers of Fe^{2+} and Fe^{3+} ions with as a consequence, a maximum of conductivity.

The observatons of $\sigma = f(t)$ curves in a variety of ferrous spinels with Fe^{2+} ions on A sites, suggest that these curves could be represented by the scheme shown in Fig. 12 with a maximum for $t = t_0$. That conclusion is supported by observations made for solid solutions $(Fe^{2+}Al_{2-x}^{3+}Cr_x^{3+})O_4^{2-}$ with $x = 1.5$ (Fig. 5) and for chromium-substituted magnetites with $x \geqslant 1.80$ (Fig. 4). In order to achieve this behaviour, we may make a comparison between theoretical and experimental curves (Fig. 13). The experimental curve shows the evolution of transformation rates α and α' with oxidation time on both sides of the maximum leading to the expressions:

$$\alpha = \sigma_{(t)} - \sigma_{(o)}/\sigma_{(m)} - \sigma_{(o)} \quad \text{and}$$

$$\alpha = \sigma_{(t)} - \sigma_{(f)}/\sigma_{(m)} - \sigma_{(f)}$$

where $\sigma_{(m)}$ is the conductivity at time t_0. The theoretical curves were computed for various values of $\tilde{D}$ from the diffusion Equations 6 and 7 which are obeyed in the two media.

The comparison between experimental and theoretical curves suggests that the diffusion coefficient varies as the reaction proceeds with the number of $Fe^{2+}-Fe^{3+}$ pairs. The diffusion analysis is somewhat

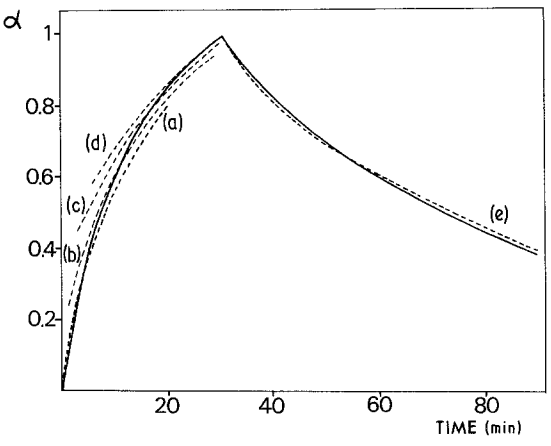

Figure 13 Comparison of theoretical (– – –) and experimental (—) curves; (a) $D = 1.1 \times 10^{-15}\,cm^2\,sec^{-1}$; (b) $D = 1.5 \times 10^{-15}\,cm^2\,sec^{-1}$; (c) $D = 1.9 \times 10^{-15}\,cm^2\,sec^{-1}$; (d) $D = 2.2 \times 10^{-15}\,cm^2\,sec^{-1}$; (e) $D = 2 \times 10^{-16}\,cm^2\,sec^{-1}$.

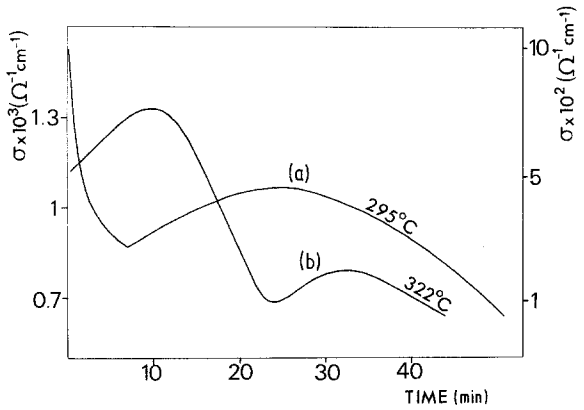

Figure 14 Evolution of electrical conductivity with time for spinels with Fe^{2+} ions on both sites. (a) Chromium-substituted magnetite with $x = 1.20$, (b) titanium-substituted magnetite with $x = 0.82$.

more intricate but it shows that:

(a) the diffusion coefficient increases with the concentration of $Fe^{2+}-Fe^{3+}$ pairs, hence a general method must be considered including, for example, an unsteady-state diffusion with moving boundary [13];

(b) the process of oxidation may cause changes in the crystal lattice parameter. For iron chromite this change is of the order of 0.012 nm which involves higher stresses inside the solid.

3.3. Case of spinels with Fe^{2+} ions on both sites

In the study of the oxidation process discussed above, the Fe^{2+} ions are located on B or A sites and these spinels were chosen as examples of those containing, after oxidation, iron ions at the B sites (as Fe_3O_4) or at the A sites only (as $FeCr_2O_4$). In order to extend the understanding of the electron exchange process within spinels we have tentatively explained the electrical behaviour of mixed ferrous spinels whose Fe^{2+} ions are present on both sites but with foreign cations. We selected two systems, $Fe_{3-x}Cr_xO_4$ and $Fe_{3-x}Ti_xO_4$. For $x = 1.20$, chromium-substituted magnetite has the cation distribution: $(Fe_{0.7}^{2+}Fe_{0.3}^{3+})_A(Fe_{0.3}^{2+}Fe_{0.5}^{3+}Cr_{1.2}^{3+})_BO_4^{2-}$ and for $x = 0.82$, titanomagnetite can be structurally formulated as: $(Fe_{0.72}^{2+}Fe_{0.28}^{3+})_A(Fe_{1.00}^{2+}Fe_{0.12}^{3+}Ti_{0.82}^{4+})_AO_4^{2-}$. This spinel can be regarded as chromium-substituted magnetite in which Cr^{3+} has been completely replaced by Ti^{4+}.

In both cases the plots of σ against time display a two-stage oxidation process (Fig. 14). This behaviour can be explained as follows: for chromium-substituted magnetites (Fig. 14a) the Fe^{2+} ions on B sites are oxidized preferentially, producing a decrease of conductivity since initially the Fe^{2+} ions are fewer than Fe^{3+} ions, thus decreasing the number of $Fe^{2+}-Fe^{3+}$ pairs. Then the Fe^{2+} ions on A sites, which are initially more numerous, are in time oxidized which favours electron exchange between Fe^{2+} and Fe^{3+} ions present on equivalent sites, here A sites. Finally, the conductivity decreases as for inverse spinels. In the case of titanium-substituted magnetite (Fig. 14b) a maximum of conductivity corresponding to a maximum of $Fe^{2+}-Fe^{3+}$ pairs on A and B sites, respectively, can be detected when the Fe^{2+} concentration is equal to that of Fe^{3+} ions. Such an observation clearly

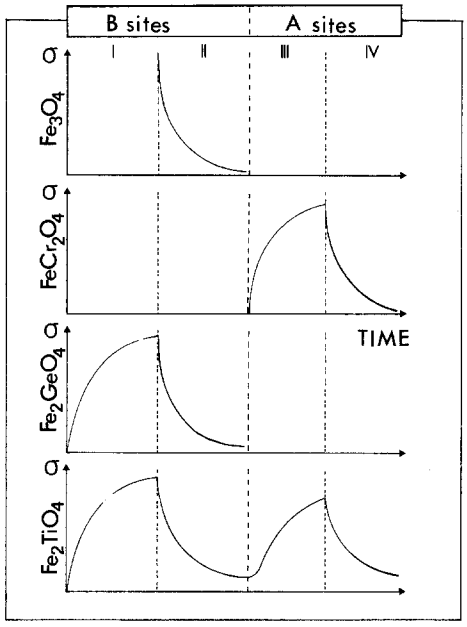

Figure 15 Schematic illustration of the evolution of electrical conductivity with time for different ferrous spinels.

suggests the important role played by the location of Fe^{2+} ions in spinel structure during oxidation at low temperature. We will not attempt to pursue here these examples, but mainly point out that the behaviour of electrical conductivity can be predicted from the knowledge of the content and distribution of Fe^{2+} cations amongst octahedral B and tetrahedral A occupied sites. A schematic interpretation of the evolution of electrical conductivity is given in Fig. 15 for different cation distributions. Restricting the analysis to the location of Fe^{2+} ions in spinel lattice and ignoring the presence of foreign cations, four domains can be distinguished in the function of the evolution of the Fe^{2+}/Fe^{3+} ration in each site. If the number of $Fe^{2+}-Fe^{3+}$ pairs is the only process involved in the change of conductivity during oxidation, domains I and II are associated with the change in the number of $Fe^{2+}-Fe^{3+}$ pairs in the B sites and domains III and IV with change of $Fe^{2+}-Fe^{3+}$ pairs in the A sites because thermogravimetric studies have suggested that oxidation of B sites iron will be more rapid than A sites iron. It follows that for some ferrous spinels we can predict the domains corresponding to the variation with time as shown in Fig. 15.

We will now discuss the change of conductivity with time. $FeCr_2O_4$ containing all iron in the A sites undergoes a maximum of conductivity between III and IV domains. For Fe_3O_4 only domain II is observed. In contrast, for Fe_2TiO_4 with structural formula $(Fe^{2+})_A(Fe^{2+}Ti^{4+})_BO_4^{2-}$, the four domains are found. Moreover, if our hypothesis is correct, the evolution of conductivity of $GeFe_2O_4$ containing all iron in the B sites can be represented by domains I and II.

4. Conclusion

To compare with thermogravimetric data, a relation between the ionic diffusion of Fe^{2+} ions and evolution of the number of $Fe^{2+}-Fe^{3+}$ pairs has been established from the two cation sites of the spinel structure represented by Fe_3O_4 and $FeCr_2O_4$ where all iron cations are on B or A sites. The mechanism of bulk oxidation of these spinels is now probably the best supported model to account for the electrical behaviour with the Fe^{2+} concentration where these ions are distributed on unequal sites. This mechanism, which considers an electron exchange between Fe^{2+} and Fe^{3+} ions on both sites, also accounts for observations of discrepancy in reactivity as a function of the initial cation distribution or diffusion process. In each case the electrical behaviour supports the kinetic interpretation of structure sensitivity, the only condition being the maintenance of spinel structure during oxidation, resulting in a change in stoichiometry with conservation of the oxygen lattice resulting in defect phases, γ, without the generation of other phases. Under these conditions σ reflects the effect of the degree of oxidation α.

This electron "hopping" behaviour is also observed in a variety of other ferrous spinels, varying with the distribution of Fe^{2+} ions and the ratio of Fe^{2+} to Fe^{3+} due to incorporation of foreign cations. The results, however, can be discussed only qualitatively and we are currently working to develop a more quantitative picture of the possible processes in this and similar compounds. For example, it is possible that Cr^{3+} or Ti^{4+} ions, which distinctly prefer octahedral positions, will also play a role in the mechanism of conduction because one may assume rearrangements of the type

$$n\mathrm{Fe}^{3+} + m\mathrm{Ti}^{3+} = n\mathrm{Fe}^{2+} + m\mathrm{Ti}^{4+},$$

i.e. the mechanism of controlled valence with the aid of admixture ions [14].

References

1. B. GILLOT, F. CHASSAGNEUX and A. ROUSSET, *J. Solid State Chem.* **38** (1981) 219.
2. B. GILLOT, F. JEMMALI, F. CHASSAGNEUX, C. SALVAING and A. ROUSSET, *ibid.* **45** (1982) 317.
3. B. GILLOT, F. JEMMALI, L. CLERC and A. ROUSSET, *C. R. Acad. Sci., Paris Serie II* **302** (1986) 211.
4. A. ROUSSET, P. GERMI and J. PARIS, *Ann. Chim. Fr.* **7** (1972) 57.
5. P. MOLLARD, A. COLLOMB, J. DEVENYI, A. ROUSSET and J. PARIS, *IEEE Trans. Mag. Mag.* **11** (1975) 894.
6. F. CHASSAGNEUX and A. ROUSSET, *J. Solid State Chem.* **16** (1976) 161.
7. B. GILLOT and J. F. FERRIOT, *J. Phys. Chem. Solids* **37** (1976) 857.
8. R. GERARDIN, A. RAMDANI, C. GLEITZER, B. GILLOT and B. DURAND, *J. Solid State Chem.* **57** (1985) 215.
9. F. A. KRÖGER, "The Chemistry of Imperfect Crystals" (North-Holland, Amsterdam, 1964) p. 996.
10. B. GILLOT, D. DELAFOSSE and P. BARRET, *Mat. Res. Bull.* **8** (1973) 1431.
11. B. GILLOT, R. M. BENLOUCIF and A. ROUSSET, *J. Phys. Chem. Solids* **42** (1981) 209.
12. B. GILLOT, R. M. BENLOUCIF and A. ROUSSET, *Mat. Res. Bull.* **16** (1981) 481.
13. P. V. DANCKWERTS, *Trans. Faraday Soc.* **46** (1950) 701.
14. J. BROZ, S. KRUPICKA and K. ZAVETA, *Czech. J. Phys.* **9** (1959) 481.

Received 10 February
and accepted 10 April 1986